

Bottinoite, $\text{Ni}(\text{H}_2\text{O})_6[\text{Sb}(\text{OH})_6]_2$: Crystal structure, twinning, and hydrogen-bond model

PAOLA BONAZZI¹ AND FIORENZO MAZZI²

¹Dipartimento di Scienze della Terra, Università di Firenze, via La Pira 4, I-50121 Florence, Italy

²CNR-CS Cristallografia e la Cristallografia, Dipartimento di Scienze della Terra, Università di Pavia, via Abbiategrasso 209, I-27100 Pavia, Italy

ABSTRACT

The crystal structure of bottinoite, $\text{Ni}(\text{H}_2\text{O})_6[\text{Sb}(\text{OH})_6]_2$, was determined from a twinned crystal. This study revealed that the strong $\bar{3}1m$ pseudosymmetry shown by all the natural and synthetic crystals examined results from $\{10\bar{1}0\}$ twinning. The structure is trigonal (space group $P3$) with $a = 16.045(4)$, $c = 9.784(2)$ Å (natural bottinoite) and $a = 16.060(3)$, $c = 9.792(1)$ Å (synthetic analog). The structure consists of a sequence of pairs of layers parallel to (0001) and stacked along the c axis. Each layer consists of isolated octahedra, linked together by hydrogen bonds, which also connect adjacent layers. Ni^{2+} cations are ordered in two of the ten independent octahedral sites in one layer, whereas the second layer of the pair is made up of only Sb^{5+} octahedra. The average octahedral bond lengths are 2.06 and 1.98 Å for NiO_6 and SbO_6 , respectively. The ten independent octahedra show four orientations mutually related by pseudosymmetry operations. This particular feature is taken into account in the formulation of a hydrogen-bonding model and a twinning mechanism. Structural and geometrical relationships with the brucite-like $\text{M}^{2+}(\text{OH})_2$ structures are also discussed.

INTRODUCTION

Bottinoite, $\text{Ni}(\text{H}_2\text{O})_6[\text{Sb}(\text{OH})_6]_2$, was first found at the Bottino Mine, Apuan Alps, Italy (Bonazzi et al. 1992), as an alteration product of ullmannite. Thus far, the mineral was reported by Clark (1993) from three localities in the British Isles; the association with ullmannite is common to all known occurrences of this mineral.

On the basis of its chemical composition, lattice parameters, and powder pattern, bottinoite was found to correspond to the synthetic product studied by Beintema (1936). In agreement with observations by this author, Bonazzi et al. (1992) stated that all the crystals examined showed a Laue symmetry of $\bar{3}m$, with no systematic extinctions, and $I_{hkl} = I_{khl} \neq I_{h\bar{k}\bar{l}}$. Space group choices were therefore $P\bar{3}1m$, $P31m$, and $P312$. Attempts to solve the crystal structure were made on both synthetic and natural crystals, starting from the structural model hypothesized by Beintema (1936) and taking into account the lattice relationships to brucite-like structures. However, the crystal structure of bottinoite remained unsolved. The hypothesis that the presence of twinning could be the reason for the failure of the previous attempts was the starting point of the present study.

EXPERIMENTAL METHODS

A crystal of bottinoite (BN1) from the Bottino mine and one of its synthetic analogs (BS2) obtained following the procedure described by Beintema (1936) were selected to collect intensity data. Diffraction quality was tested by means of the Weissenberg technique. Diffraction spots

appeared somewhat broad (especially for BN1), but no extra reflections were observed on the films. The unit-cell dimensions for both crystals, determined by least-squares refinement using 25 centered reflections ($25.0^\circ < \theta < 28.4^\circ$) measured on a CAD4 diffractometer, are $a = 16.045(4)$, $c = 9.784(2)$ Å (BN1), and $a = 16.060(3)$, $c = 9.792(1)$ Å (BS2).

Intensity data were collected and subsequently corrected for Lorentz-polarization effects and for absorption using the semiempirical method of North et al. (1968). Experimental details are reported in Table 1.

STRUCTURE SOLUTION AND REFINEMENT

The analysis of the intensity data sets for both crystals confirmed an apparent Laue symmetry of $\bar{3}m$. Statistical tests on the distribution of $|E|$ values indicated the absence of an inversion center, in agreement with the observation of a second-order nonlinear susceptibility reported by Bonazzi et al. (1992). Therefore, direct methods were tentatively used with the two probable space groups for bottinoite, $P\bar{3}1m$ and $P312$. In both cases, peaks attributable to metal atoms were located on the F_o -Fourier map, at all vertices of a subcell $\frac{1}{3}[100]$, $\frac{1}{3}[010]$, $\frac{1}{3}[001]$. However, attempts to refine O atoms located on successive ΔF -Fourier maps were unsuccessful. A careful examination of the Patterson map revealed that the orientation of MeO_6 ($\text{Me} = \text{Sb}, \text{Ni}$) octahedra in bottinoite is not consistent with the symmetry operators of $P\bar{3}1m$ and $P312$; in fact, for the latter space group, octahedra can be oriented according to the Patterson indication only if z/c of Me at-

TABLE 1. Crystal data and experimental details

	BN1	BS2
Crystal system	trigonal	trigonal
Space group	$P\bar{3}$	$P\bar{3}$
Cell parameters		
a (Å)	16.045(4)	16.060(3)
c (Å)	9.784(2)	9.792(1)
V (Å ³)	2181.4(9)	2187.2(6)
Z	6	6
Crystal size (μm)	50 × 200 × 220	100 × 290 × 300
θ range (°)	2–30	2–30
Scan mode, scan width	ω , 2.2°	ω , 2.2°
Scan speed (°/min)	1.3–3.3	1.6–3.3
Range of hkl	–23, 23 –23, h 0, 13	–23, 23 –23, h 0, 13
No. of collected refl.	6584	6840
Refl. used for ψ -scan	1 7 2	–6 12 2
Relative χ angle (°)	88.5	87.1
Min. transmission (%)	68.8	51.2
Max. transmission (%)	99.9	99.7
No. of independent refl.	4085	4269
No. of observed refl. ($I_{\text{obs}} > 3\sigma$)	2304	3225
R_{obs} (%)	4.0	3.5
Final $\Delta\rho_{\text{min}}$ (e/Å)	–2.8	–1.3
Final $\Delta\rho_{\text{max}}$ (e/Å)	1.3	4.0

oms is $\frac{1}{4}$ and $\frac{3}{4}$ instead of 0 and $\frac{1}{2}$. This last structural model, however, was checked without success. The presence of $\{10\bar{1}0\}$ twinning in crystals with $P\bar{3}$ (or $P\bar{3}$) symmetry was then considered. To explain the apparent $\bar{3}1m$ symmetry, the proportion of each component of the twinned crystal was supposed to be about 50%. If such twinning takes place, all reflections of the first component overlap with those of the second with Miller indices hkl and $h\bar{h}l$, respectively. The structure refinement was performed using a locally modified version of the program ORFLS (Busing et al. 1962) that was adapted for twinned crystal structures and allows the fraction of the twin component to be refined. To evaluate the most reliable Sb-Ni distribution among those possible in $P\bar{3}$ (or $P\bar{3}$), several least-squares cycles were initially run with only the metal atoms (coordinates as derived from direct methods). The O atoms were then located on the ΔF -Fourier map. Refinements in the centrosymmetric model ($P\bar{3}$) did not achieve convergence, and the displacement parameters for the atoms located on symmetry centers were unreliable. On the contrary, in the $P\bar{3}$ space group, the structural refinement converged to $R = 3.5\%$ for the 3225 reflections with $I > 3\sigma$, and 6.7% for all 4269 reflections (BS2 crystal). For the BN1 crystal, $R = 4.0\%$ for 2304 reflections with $I > 3\sigma$, and 10.1% for all 4085 reflections. The refined value of the twin component was 50% for BS2 and 51% for BN1. The precision of the refined parameters was improved by using all the data (previously merged in $\bar{3}1m$ symmetry) and fixing the twin proportion to 50%. H atoms were added, but their coordinates and displacement parameters were fixed during refinement (see below). The final unweighted R value for all reflections with $I > 0$ was 4.6% ($N_{\text{ref}} = 4269$) and 7.1% ($N_{\text{ref}} = 4085$) for BS2 and BN1, respectively. A unit-weighting scheme was applied during the least-squares refinement. Scattering curves were taken from the *International Tables of Crystallography*, vol. IV (Ibers

and Hamilton 1974). Atomic coordinates and equivalent isotropic displacement factors for BS2 and BN1 are listed in Tables 2 and 3, respectively. Table 4 reports the anisotropic displacement parameters, and Table 5 reports the observed and calculated structure factors for BS2 and BN1.¹

DESCRIPTION OF THE STRUCTURE

The structure of bottinoite consists of a sequence of layers parallel to (0001) and stacked along the c axis. Each layer consists of isolated octahedra, linked together by hydrogen bonds, which also connect the adjacent layers. The structure can also be described as a nearly hexagonal close-packed array of O atoms (stacking sequence ABA'B') with metal atoms in one-sixth of the octahedral interstices. Planes of unfilled octahedral cavities ($z \approx \frac{1}{4}$ and $z \approx \frac{3}{4}$) alternate with planes of metal atoms ordered on one-third of the octahedral sites ($z \approx 0$ and $z \approx \frac{1}{2}$). In particular, at $z \approx 0$, two-ninths of the octahedral sites are occupied by Ni²⁺ and one-ninth are occupied by Sb⁵⁺ (Fig. 1a); at $z \approx \frac{1}{2}$, one-third of the octahedral sites are occupied solely by Sb⁵⁺ (Fig. 1b).

Synthetic and natural bottinoite show identical structural connectivity and the same Ni-Sb distribution, with only minor changes in individual bond lengths and bond angles (differences are within $\pm 2\sigma$). Therefore, in the discussion that follows, reference is made only to the structure of the synthetic compound (BS2). The bond distances and angles for BS2 are reported in Table 6. The average $\langle \text{Sb-O} \rangle$ bond length of 1.98 Å compares well with other minerals containing Sb⁵⁺(O,OH)₆ octahedra: 1.97 Å in richelsdorfite (Süsse and Tillmann 1987), 1.98 Å in mam-

¹ A copy of Tables 4 and 5 may be ordered as Document AM-96-628 from the Business Office, Mineralogical Society of America, 1015 Eighteenth Street NW, Suite 601, Washington, DC 20036, U.S.A. Please remit \$5.00 in advance for the microfiche.

TABLE 2. Fractional atomic coordinates and isotropic displacement parameters for synthetic bottinoite

	<i>x/a</i>	<i>y/b</i>	<i>z/c</i>	<i>B_{eq}</i> (Å ²)
Layer at <i>z</i> ≈ 0				
Sb1	0	0	0.0000*	1.0(1)
Sb2	⅓	⅓	-0.0883(2)	0.7(1)
Sb3	⅓	⅓	-0.0021(6)	1.4(1)
Ni1	0.3379(2)	0.0080(2)	-0.0311(5)	1.2(1)
Ni2	0.6639(3)	-0.0065(2)	-0.0505(4)	0.9(1)
O1	0.032(1)	0.117(1)	-0.120(2)	2.3(5)
O2	0.114(1)	0.081(1)	0.112(1)	2.3(5)
O3	0.579(1)	0.221(1)	-0.200(2)	2.4(4)
O4	0.697(1)	0.254(1)	0.027(1)	1.1(4)
O5	0.302(1)	0.554(1)	0.119(1)	1.1(4)
O6	0.364(1)	0.783(1)	-0.109(1)	1.3(4)
O7	0.315(1)	0.097(1)	-0.159(2)	2.0(5)
O8	0.426(1)	0.116(1)	0.093(1)	1.4(4)
O9	0.454(1)	0.036(1)	-0.147(2)	1.9(4)
O10	0.363(1)	-0.085(1)	0.088(2)	1.5(5)
O11	0.253(1)	-0.107(1)	-0.156(1)	1.2(4)
O12	0.215(1)	-0.028(1)	0.091(2)	2.1(5)
O13	0.582(1)	0.027(2)	0.070(2)	2.2(6)
O14	0.693(1)	0.111(1)	-0.160(1)	1.1(4)
O15	0.781(1)	0.081(1)	0.070(2)	2.0(5)
O16	0.754(1)	-0.032(2)	-0.178(2)	2.8(6)
O17	0.633(1)	-0.126(1)	0.067(1)	2.1(4)
O18	0.553(1)	-0.091(1)	-0.172(2)	2.4(4)
Layer at <i>z</i> ≈ ½				
Sb4	0	0	0.4974(3)	0.8(1)
Sb5	⅓	⅓	0.4185(2)	1.0(1)
Sb6	⅓	⅓	0.4987(3)	0.9(1)
Sb7	0.3283(1)	-0.0066(1)	0.4704(4)	1.0(1)
Sb8	0.6678(2)	0.0055(1)	0.4496(2)	0.7(1)
O19	0.064(1)	0.112(1)	0.366(2)	1.9(4)
O20	0.115(1)	0.042(1)	0.611(2)	1.6(4)
O21	0.550(1)	0.269(1)	0.535(1)	0.4(2)
O22	0.623(1)	0.220(1)	0.302(1)	1.5(5)
O23	0.263(1)	0.550(1)	0.615(1)	0.9(3)
O24	0.395(1)	0.778(1)	0.377(2)	1.8(4)
O25	0.260(1)	0.039(1)	0.344(2)	1.7(5)
O26	0.378(1)	0.113(1)	0.578(1)	0.7(3)
O27	0.447(1)	0.060(1)	0.347(1)	1.4(4)
O28	0.400(1)	-0.050(1)	0.585(1)	1.0(4)
O29	0.281(1)	-0.123(1)	0.346(1)	1.0(4)
O30	0.211(1)	-0.074(1)	0.581(1)	1.1(4)
O31	0.618(1)	0.074(1)	0.567(1)	1.0(3)
O32	0.732(1)	0.116(1)	0.326(1)	1.7(5)
O33	0.779(1)	0.055(1)	0.562(1)	1.3(4)
O34	0.707(1)	-0.067(1)	0.330(2)	2.1(5)
O35	0.607(1)	-0.108(1)	0.567(1)	0.9(3)
O36	0.551(1)	-0.040(1)	0.337(2)	1.4(4)

* Fixed during refinement.

TABLE 3. Fractional atomic coordinates and isotropic displacement parameters for natural bottinoite

	<i>x/a</i>	<i>y/b</i>	<i>z/c</i>	<i>B_{eq}</i> (Å ²)
Layer at <i>z</i> ≈ 0				
Sb1	0	0	0.0000*	1.0(1)
Sb2	⅓	⅓	-0.0888(3)	0.5(1)
Sb3	⅓	⅓	0.0002(5)	1.9(1)
Ni1	0.3372(4)	0.0100(3)	-0.0368(5)	1.4(1)
Ni2	0.6605(4)	-0.0066(4)	-0.0524(4)	1.5(1)
O1	0.033(2)	0.118(2)	-0.118(3)	2.1(8)
O2	0.114(2)	0.084(2)	0.109(2)	2.2(9)
O3	0.581(1)	0.221(1)	-0.202(3)	2.1(7)
O4	0.701(2)	0.257(1)	0.023(2)	1.0(5)
O5	0.302(2)	0.554(2)	0.118(2)	1.2(6)
O6	0.360(2)	0.779(1)	-0.111(2)	1.3(6)
O7	0.316(3)	0.099(2)	-0.158(2)	3.7(9)
O8	0.425(2)	0.114(2)	0.099(2)	1.8(8)
O9	0.452(2)	0.034(2)	-0.152(3)	2.0(7)
O10	0.365(2)	-0.085(2)	0.083(3)	1.9(7)
O11	0.254(2)	-0.108(2)	-0.160(3)	1.9(6)
O12	0.216(2)	-0.025(2)	0.088(3)	1.9(8)
O13	0.580(2)	0.023(3)	0.068(2)	2.2(9)
O14	0.697(2)	0.110(2)	-0.165(2)	1.2(6)
O15	0.778(2)	0.080(2)	0.067(2)	1.8(8)
O16	0.755(2)	-0.026(3)	-0.175(3)	2.8(9)
O17	0.631(2)	-0.128(2)	0.066(2)	1.3(5)
O18	0.551(2)	-0.092(2)	-0.169(2)	2.0(6)
Layer at <i>z</i> ≈ ½				
Sb4	0	0	0.4943(5)	0.9(1)
Sb5	⅓	⅓	0.4193(4)	1.1(1)
Sb6	⅓	⅓	0.5037(4)	0.6(1)
Sb7	0.3273(2)	-0.0066(2)	0.4706(4)	1.1(1)
Sb8	0.6679(2)	0.0052(1)	0.4501(2)	0.7(1)
O19	0.057(2)	0.109(1)	0.368(2)	1.7(6)
O20	0.116(2)	0.041(2)	0.610(2)	1.5(6)
O21	0.550(1)	0.264(1)	0.537(2)	0.5(3)
O22	0.620(2)	0.221(2)	0.299(2)	1.4(6)
O23	0.261(1)	0.550(1)	0.613(2)	0.9(5)
O24	0.393(2)	0.779(2)	0.379(2)	1.9(7)
O25	0.260(2)	0.038(2)	0.343(2)	1.5(7)
O26	0.375(2)	0.119(2)	0.575(2)	0.7(4)
O27	0.446(2)	0.058(2)	0.341(2)	1.4(6)
O28	0.399(2)	-0.052(2)	0.582(2)	0.8(5)
O29	0.280(2)	-0.123(2)	0.348(2)	1.5(6)
O30	0.214(2)	-0.070(2)	0.582(2)	0.9(4)
O31	0.619(1)	0.072(2)	0.568(2)	0.9(5)
O32	0.736(2)	0.117(2)	0.326(2)	2.1(8)
O33	0.783(2)	0.057(2)	0.557(2)	1.3(6)
O34	0.710(2)	-0.062(2)	0.323(2)	1.6(7)
O35	0.608(2)	-0.106(2)	0.563(2)	1.1(5)
O36	0.550(2)	-0.042(2)	0.333(2)	1.3(6)

* Fixed during refinement.

mothite (Effenberger 1985), 1.99 Å in shakhovite (Tillmanns et al. 1982) and manganostibite (Moore 1970), 1.97 and 1.99 Å in bahianite (Moore and Araki 1976), and 2.00 Å in monoclinic langbanite (Giuseppetti et al. 1991). The mean bond distances of $\langle \text{Ni1-O} \rangle = 2.065$ Å and $\langle \text{Ni2-O} \rangle = 2.045$ Å are appreciably greater than $\langle \text{Sb-O} \rangle$, consistent with the ordering of Ni in two of ten independent positions. All the octahedra are fairly regular (mean quadratic elongation ranging from 1.0010 to 1.0045) and are not flattened trigonally.

The orientation of each octahedron can be described by the angle $\phi = \sum \phi_i / 6$, where ϕ_i is the angle between the *a* axis and the projection of the Me-O_i octahedral distance on the (0001) plane. Each ϕ_i value is normalized to a value <120° by subtracting even or odd multiples of

60° according to whether the *z* value of the coordinated O_i atom is greater or less than the *z* coordinate of the metal atom. The ϕ angles for the ten independent octahedra cluster around the four values, 24.2(±1.4), 45.1(±2.6), 73.4(±2.5), and 95.7(±1.7)°, which are labeled d, b, p, and q, respectively (Fig. 2). In the layer at *z* ≈ 0, the octahedra assume b and p orientations, whereas in the layer at *z* ≈ ½, d and q replace b and p. A strong 1*m* pseudosymmetry relates the octahedral orientation b to p and d to q; in fact, the values b + p (118.5°) and d + q (119.9°) are close to the theoretical value of 120° required to transform b into p and d into q by means of a (10 $\bar{1}$ 0) reflection. This hidden symmetry, which correlates the octahedral orientations into pairs but is not present in the structure, could be the cause of the {10 $\bar{1}$ 0}

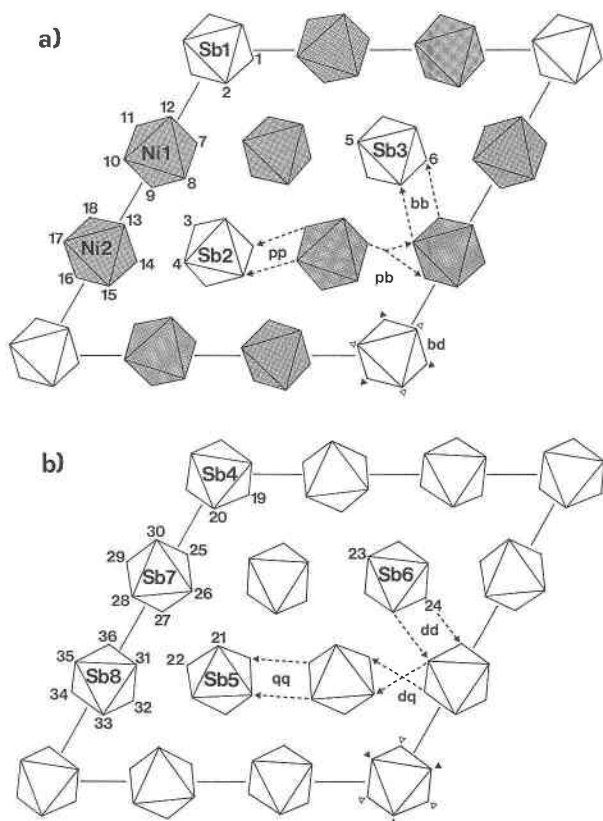


FIGURE 1. Octahedral layers at $z \approx 0$ (a) and $z \approx 1/2$ (b). Sb octahedra are white, Ni octahedra are gray. Labels concern the atoms of the asymmetric unit. Examples of hydrogen bonding between octahedra in various orientations are also drawn. Hydrogen bonds occurring between adjacent layers are symbolized by triangles showing one vertex or one edge near the octahedral vertices for acceptor or donor O atoms, respectively. Open triangles represent hydrogen bonds directed upward, and solid triangles represent hydrogen bonds directed downward.

twinning in bottinoite. Furthermore, as emphasized by the choice of the labels d, b, p, and q, a twofold pseudosymmetry along the [0001] axis transforms b to q and p to d, whereas a $(\bar{1}210)$ pseudomirror transforms b to d and p to q. In the $P3$ space group, however, there are no symmetry constraints limiting the orientation of the octahedra. Nevertheless, there are only four values for the ϕ angle. The reason for this becomes clear when one considers the O ... O contacts between octahedra belonging to the same layer. The O ... O distances between two equally oriented octahedra $(x,y,z$ and $x + 1/3,y + 1/3,z - \Delta z$, with Δz ranging between 0 and 0.05) were computed as a function of ϕ . From this calculation, only four ranges of values for the ϕ angle were found that maintained two O ... O contacts of suitable length (2.6–2.8 Å) for donor-acceptor distances: 15–25° (d), 35–45°(b), 75–85°(p), and 95–105°(q). Analogously, it can be explained why the octahedra belonging to adjacent layers are stacked on top of each other with different orientations: Stackings such

TABLE 6. Selected bond distances (Å) and angles (°) for synthetic bottinoite

Sb1-O2 (× 3)	1.97(2)	Sb4-O20 (× 3)	1.96(2)
Sb1-O1 (× 3)	2.05(2)	Sb4-O19 (× 3)	2.02(2)
⟨Sb1-O⟩	2.010	⟨Sb4-O⟩	1.990
O2-Sb1-O2 (× 3)	91.9(5)	O20-Sb4-O20 (× 3)	91.1(5)
O2-Sb1-O1 (× 3)	89.4(5)	O20-Sb4-O19 (× 3)	94.7(4)
O2-Sb1-O1 (× 3)	178.7(6)	O20-Sb4-O19 (× 3)	174.0(5)
O2-Sb1-O1 (× 3)	88.2(5)	O20-Sb4-O19 (× 3)	90.2(4)
O1-Sb1-O1 (× 3)	90.5(5)	O19-Sb4-O19 (× 3)	83.9(4)
Sb2-O4 (× 3)	1.94(1)	Sb5-O22 (× 3)	1.96(1)
Sb2-O3 (× 3)	1.97(1)	Sb5-O21 (× 3)	1.99(1)
⟨Sb2-O⟩	1.955	⟨Sb5-O⟩	1.975
O4-Sb2-O4 (× 3)	89.5(4)	O22-Sb5-O22 (× 3)	89.5(4)
O4-Sb2-O3 (× 3)	87.1(5)	O22-Sb5-O21 (× 3)	87.8(4)
O4-Sb2-O3 (× 3)	91.2(4)	O22-Sb5-O21 (× 3)	92.6(3)
O4-Sb2-O3 (× 3)	176.5(5)	O22-Sb5-O21 (× 3)	176.6(4)
O3-Sb2-O3 (× 3)	92.2(4)	O21-Sb5-O21 (× 3)	90.3(3)
Sb3-O6 (× 3)	1.98(1)	Sb6-O24 (× 3)	1.96(1)
Sb3-O5 (× 3)	2.00(1)	Sb6-O23 (× 3)	1.99(1)
⟨Sb3-O⟩	1.990	⟨Sb6-O⟩	1.975
O6-Sb3-O6 (× 3)	94.6(4)	O24-Sb6-O24 (× 3)	86.8(4)
O6-Sb3-O5 (× 3)	87.8(4)	O24-Sb6-O23 (× 3)	89.6(4)
O6-Sb3-O5 (× 3)	88.9(4)	O24-Sb6-O23 (× 3)	93.2(4)
O5-Sb3-O5 (× 3)	175.7(4)	O23-Sb6-O23 (× 3)	176.3(4)
O5-Sb3-O5 (× 3)	88.6(3)	O23-Sb6-O23 (× 3)	90.6(3)
Ni1-O8	2.01(1)	Sb7-O30	1.96(1)
Ni1-O9	2.03(1)	Sb7-O26	1.97(1)
Ni1-O11	2.06(1)	Sb7-O28	1.97(1)
Ni1-O7	2.07(2)	Sb7-O25	2.02(1)
Ni1-O10	2.09(1)	Sb7-O29	2.03(1)
Ni1-O12	2.13(2)	Sb7-O27	2.05(1)
⟨Ni1-O⟩	2.065	⟨Sb7-O⟩	2.000
O8-Ni1-O9	88.5(4)	O30-Sb7-O26	93.0(4)
O8-Ni1-O11	176.2(5)	O30-Sb7-O28	93.5(4)
O8-Ni1-O7	93.5(4)	O30-Sb7-O25	89.6(4)
O8-Ni1-O10	88.6(4)	O30-Sb7-O29	90.5(4)
O8-Ni1-O12	93.0(4)	O30-Sb7-O27	177.3(4)
O9-Ni1-O11	89.4(4)	O26-Sb7-O28	91.0(3)
O9-Ni1-O7	88.3(5)	O26-Sb7-O25	90.2(3)
O9-Ni1-O10	89.2(4)	O26-Sb7-O29	175.4(4)
O9-Ni1-O12	177.3(5)	O26-Sb7-O27	89.4(4)
O11-Ni1-O7	89.6(5)	O28-Sb7-O25	176.7(4)
O11-Ni1-O10	88.2(5)	O28-Sb7-O29	91.8(3)
O11-Ni1-O12	88.9(4)	O28-Sb7-O27	88.0(4)
O7-Ni1-O10	176.7(5)	O25-Sb7-O29	86.9(3)
O7-Ni1-O12	93.8(5)	O25-Sb7-O27	88.9(4)
O10-Ni1-O12	88.7(6)	O29-Sb7-O27	87.1(4)
Ni2-O18	2.00(1)	Sb8-O33	1.90(1)
Ni2-O14	2.01(1)	Sb8-O35	1.95(1)
Ni2-O13	2.03(2)	Sb8-O32	1.96(1)
Ni2-O15	2.06(1)	Sb8-O34	1.96(2)
Ni2-O17	2.07(2)	Sb8-O36	1.97(2)
Ni2-O16	2.10(2)	Sb8-O31	2.01(1)
⟨Ni2-O⟩	2.045	⟨Sb8-O⟩	1.958
O18-Ni2-O14	91.7(5)	O33-Sb8-O35	88.6(4)
O18-Ni2-O13	92.9(4)	O33-Sb8-O32	91.1(4)
O18-Ni2-O15	178.3(5)	O33-Sb8-O34	94.6(5)
O18-Ni2-O17	89.0(5)	O33-Sb8-O36	176.7(4)
O18-Ni2-O16	88.9(4)	O33-Sb8-O31	89.3(4)
O14-Ni2-O13	86.5(4)	O35-Sb8-O32	176.9(4)
O14-Ni2-O15	87.8(5)	O35-Sb8-O34	87.5(3)
O14-Ni2-O17	178.4(5)	O35-Sb8-O36	92.5(5)
O14-Ni2-O16	90.4(4)	O35-Sb8-O31	91.4(3)
O13-Ni2-O15	88.7(4)	O32-Sb8-O34	89.4(4)
O13-Ni2-O17	92.1(4)	O32-Sb8-O36	87.9(4)
O13-Ni2-O16	176.4(5)	O32-Sb8-O31	91.8(3)
O15-Ni2-O17	91.6(5)	O34-Sb8-O36	88.5(5)
O15-Ni2-O16	89.5(5)	O34-Sb8-O31	175.9(5)
O17-Ni2-O16	91.1(4)	O36-Sb8-O31	87.6(5)

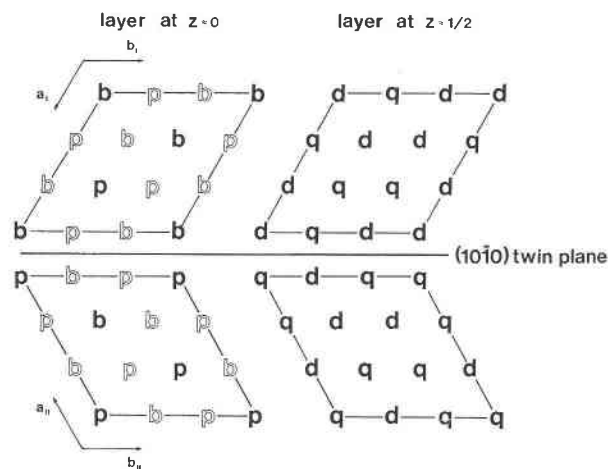


FIGURE 2. Mutual orientation of octahedra in the twinned structure of bottinoite. The octahedral orientations are schematically indicated with letters to show the observed pseudosymmetries (see text). Solid letters refer to Sb octahedra, open letters refer to Ni octahedra.

as dd (or bb, pp, qq) would involve three O ... O distances of about 3.05 Å for each pair of octahedra, which is usually too large for hydrogen bonding. Stacking between b and p is also excluded because it involves only bp and pb contacts in all the layers, without the possibility to differentiate between the layer containing Ni + Sb and the one containing only Sb. The remaining stacking sequences involve bd (and pq) or bq (and pd). The former (three O ... O contacts of about 2.8 Å) leads to a Me-O ... O angle of 115°, which is closer to the theoretical tetrahedral angle than that (124°) calculated for a bq (and pd) contact (three O ... O contacts of about 2.6 Å). Indeed, we observed only b-d-b-d and p-q-p-q sequences along [0001]. There are 54 contacts (three for each of the ten octahedral bd pairs and the eight pq pairs) between O atoms belonging to adjacent layers. Of the 144 H atoms in bottinoite, $\text{Ni}(\text{H}_2\text{O})_6[\text{Sb}(\text{OH})_6]_2$ ($Z = 6$), 54 are located in connecting adjacent layers, whereas the other 90 provide linkages between octahedra within the layers.

Finally, it can be explained why each layer is not made up of octahedra in the same orientation. If this were the case, 54 O ... O contacts suitable for hydrogen bonds would occur between 27 pairs of adjacent octahedra within each layer, more than the number required by the chemical formula. Actually, in the layer at $z \approx 1/2$, d-q couplings involve 54 O ... O contacts suitable for hydrogen bonds, whereas the connectivity within the layer at $z \approx 0$ requires only 36 H atoms. In fact, 18 H atoms are required along the O ... O contacts between equally oriented octahedra, and another 18 H atoms along the O ... O contacts in the bp couplings involve contacts suitable for bifurcated hydrogen bonds. Different couplings of octahedral orientations, such as db, dp, bq, and pq, would imply O ... O contacts shorter than 2.5 Å.

HYDROGEN-BONDING MODEL

A consequence of the insular octahedral arrangement in bottinoite is that the Ni^{2+} cations (Ni-O bond strength ranges from 0.29 to 0.39 vu) must be coordinated by H_2O molecules, while there should be OH groups around Sb^{5+} (Sb-O bond strength ranges from 0.72 to 0.97 vu). Therefore, the structure is built of alternating $\{[\text{Sb}(\text{OH})_6]_3[\text{Ni}(\text{H}_2\text{O})_6]_6\}^{9+}$ and $\{[\text{Sb}(\text{OH})_6]_9\}^{9-}$ layers. On the ΔF -Fourier map, only a few H atoms were unambiguously located. The positions of these, however, suggest that the connection between adjacent sheets is obtained by hydrogen bonds with donor O atoms belonging to the $\{[\text{Sb}(\text{OH})_6]_3[\text{Ni}(\text{H}_2\text{O})_6]_6\}^{9+}$ layer. In this layer, there is a sufficient number of H_2O molecules also to ensure the connection between octahedra belonging to the same layer. On the other hand, in the $\{[\text{Sb}(\text{OH})_6]_9\}^{9-}$ layer, all the H atoms should be engaged in hydrogen bonds lying within the sheet.

On the basis of this assumption and taking into account the effective O ... O distances, the hydrogen-bonding model reported in Table 7 was tentatively assigned. Contacts between O atoms belonging to different layers (Table 7) range from 2.65 to 2.91 Å, leading to stronger hydrogen bonds than those found in brucite, 3.218 Å (Zigan and Rothbauer 1967). Longer donor-acceptor distances occur within the layer at $z \approx 0$ (Table 7). There are two kinds of environment around the O atoms in H_2O that act as donors. The linkage between equally oriented octahedra (b-b or p-p) is obtained by hydrogen bonds with O ... O distances ranging from 2.67 to 2.75 Å, whereas the connection between octahedra having different orientation (b-p or p-b) is obtained by means of bifurcated hydrogen bonds (O ... O distances ranging from 2.87 to 3.14 Å). This distribution allows most O atoms to assume an approximately tetrahedral environment. Finally, within the layer at $z \approx 1/2$ (Table 7), the hydrogen bonds occurring between O atoms belonging to equally oriented octahedra (d-d or q-q) have O ... O distances in the range 2.68–2.79 Å, whereas longer distances (2.84–2.98 Å and exceptionally 3.05 and 3.19 Å) correspond to contacts between octahedra having different orientations (d-q or q-d).

TWINNING

It is well known that for twinning to occur a portion of the structure must be coherent with both twin-related orientations (I, II) so that the free energy at the twin boundary is a minimum. In bottinoite the twin plane (10 $\bar{1}$ 0) transforms $p_{\text{I}} \rightarrow b_{\text{II}}$, $b_{\text{I}} \rightarrow p_{\text{II}}$, $d_{\text{I}} \rightarrow q_{\text{II}}$, and $q_{\text{I}} \rightarrow d_{\text{II}}$ (Fig. 2). With regard to the layer at $z \approx 1/2$, the qdd sequence occurs in the direction of the b axis in both individuals ($x_{\text{I}} = 0, 1/3$; $x_{\text{II}} = 2/3$); the dqd sequence also is found in both twin-related structures ($x_{\text{I}} = 2/3$; $x_{\text{II}} = 0, 1/3$). Because every octahedron (d or q) is occupied by Sb, any one of these "strips" ($x = 0, x = 1/3, x = 2/3$) can constitute the twin boundary between two differently oriented individuals. Similarly, the layer at $z \approx 0$ shows the pbb

TABLE 7. Hydrogen-bonding model for synthetic bottinoite

Hydrogen bonds between adjacent layers			
O1 → O20	2.83(2) (bd)	O7 → O26	2.73(2) (pq)
O2 → O19	2.74(2) (bd)	O8 → O27	2.72(2) (pq)
O3 → O21	2.81(2) (pq)	O9 → O28	2.89(2) (pq)
O4 → O22	2.88(2) (pq)	O10 → O29	2.77(2) (pq)
O5 → O24	2.77(2) (bd)	O11 → O30	2.78(2) (pq)
O6 → O23	2.91(2) (bd)	O12 → O25	2.65(2) (pq)
			O13 → O36
			O14 → O31
			O15 → O32
			O16 → O33
			O17 → O34
			O18 → O35
			2.78(2) (bd)
			2.87(2) (bd)
			2.77(2) (bd)
			2.83(3) (bd)
			2.80(2) (bd)
			2.76(2) (bd)
Hydrogen bonds in the layer at $z \approx 0$			
O7 ↙ O14	2.92(3) (pb)	O13 ↘ O9	3.01(3) (bp)
O15 ↘ O15	3.06(3) (pb)	O10 ↙ O10	3.05(2) (bp)
O8 → O4	2.75(2) (pp)	O14 ↙ O3	3.14(2) (bp)
O9 → O3	2.68(3) (pp)	O4 ↘ O4	2.91(2) (bp)
O10 ↘ O5	3.03(3) (pb)	O15 → O2	2.72(3) (bb)
O6 ↘ O6	2.87(3) (pb)	O16 → O1	2.67(2) (bb)
O11 ↘ O16	3.08(3) (pb)	O17 → O5	2.70(2) (bb)
O17 ↘ O17	3.03(2) (pb)	O18 → O6	2.75(2) (bb)
O1 ↘ O1	2.92(3) (pb)		
O2 ↘ O2	2.93(3) (pb)		
Hydrogen bonds in the layer at $z \approx \frac{1}{2}$			
O19 → O34	2.79(3) (dd)	O25 → O19	2.96(2) (qd)
O20 → O33	2.78(2) (dd)	O26 → O21	2.68(2) (qq)
O21 → O31	2.90(2) (qd)	O27 → O22	2.74(2) (qq)
O22 → O32	2.97(3) (qd)	O28 → O23	2.98(2) (qd)
O23 → O35	2.76(2) (dd)	O29 → O24	2.98(2) (qd)
O24 → O36	2.77(2) (dd)	O30 → O20	2.97(3) (qd)
			O31 → O28
			O32 → O25
			O33 → O26
			O34 → O29
			O35 → O30
			O36 → O27
			3.05(2) (dq)
			3.19(2) (dq)
			2.93(3) (dq)
			2.98(3) (dq)
			2.94(2) (dq)
			2.84(3) (dq)

sequence ($x_I = 0, \frac{1}{3}; x_{II} = \frac{2}{3}$) and the bpp sequence ($x_I = \frac{2}{3}; x_{II} = 0, \frac{1}{3}$) in both orientations. These sequences differ for the Ni-Sb distribution, however. In the first twin component (I) pbb = Ni-Ni-Sb, and in the second component (II) pbb = Ni-Sb-Ni. The contrary happens in the bpp sequence (bpp_I = Ni-Sb-Ni, bpp_{II} = Ni-Ni-Sb). Therefore, it is probable that an accidental Ni-Sb interchange during crystal growth results in the $\{10\bar{1}0\}$ twinning in bottinoite. Furthermore, we can also assume that such defects occur so easily and frequently that each twin-related structure occurs randomly and thus constitutes about 50% of the composite crystal. All crystals examined during this study, in fact, showed a strong $31m$ pseudosymmetry, evidently related to the presence of twinned domains with the proportions close to 50%.

COMPARISON WITH BRUCITE-LIKE STRUCTURES

As reported by Bonazzi et al. (1992), the unit cell of bottinoite can be described as a supercell (54 times) of a brucite-like structure. Applying the transformation matrix $[-\frac{1}{9}, -\frac{2}{9}, 0; \frac{2}{9}, \frac{1}{9}, 0; 0, 0, \frac{1}{2}]$ to the lattice vectors of the synthetic bottinoite, a subcell with $a = 3.090$ and $c = 4.896$ Å is obtained, with a c/a ratio of 1.584, greater than that of the $M^{2+}(\text{OH})_2$ brucite-like structures. In these structures, the octahedrally coordinated sheets of O ions are flattened because of the shortening of the shared octahedral edges, and, as a consequence, the c/a ratios are considerably less than the value (1.633) calculated for an ideal HCP structure (Brindley and Kao 1984). In the brucite-like hydroxides, the value of α (= O-M-O with O ions in the same plane) is $97.4(\pm 0.4)^\circ$. In bottinoite, on the other hand, the mean value of α is 89.8° , indicating that the octahedral sheets are not flattened. Nevertheless, the c/a ratio is less than the theoretical value. This is due to the presence of unfilled sites (two-thirds within each

octahedral sheet), which leads to the expansion of the unit-cell edges parallel to (0001). This is evident from comparing the observed a parameter (3.090 Å if referred to a brucite-like cell) with the theoretical value calculated using the formula of Brindley and Kao (1984): $a = 2(M-O)\sin(\alpha/2) = 2.831$ Å, where $M-O = 2.005$ Å and $\alpha = 89.8^\circ$ (weighted averages take into account the different multiplicity of each octahedron).

The complex system of the hydrogen bonds, which requires the octahedra to assume four orientations, causes deviations from the ideal hexagonal symmetry of the array of the O atoms. In an undistorted HCP structure, the value of ϕ would be either 0 or 60° . In bottinoite, distortion is moderate in the layer at $z \approx 0$, where the Ni and Sb octahedra are rotated by -15° (b) and $+13^\circ$ (p) from the ideal position ($\phi = 60^\circ$). Greater distortion characterizes the layer at $z \approx \frac{1}{2}$, where ϕ differs from the theoretical value (0°) by 24 and -25° for d and b, respectively. The distortion of the close-packed layers is also evident from the quadratic elongation parameters (Robinson et al. 1971) of the vacant octahedral sites. In an ideal close-packed structure the vacant sites are regular (q.e. = 1.000), but in bottinoite the unoccupied octahedra have q.e. = 1.05–1.06 in the layer at $z \approx 0$ and q.e. = 1.22–1.25 in the layer at $z \approx \frac{1}{2}$. Both values are greater than those calculated for occupied Ni and Sb octahedra, which have quadratic elongation values ranging from 1.001 to 1.005.

ACKNOWLEDGMENTS

The authors thank Joanne Krueger for reading the original manuscript. This study was funded by M.U.R.S.T. (40%) and by Consiglio Nazionale delle Ricerche.

REFERENCES CITED

- Beintema, J. (1936) On the crystal-structure of magnesium- and nickel antimoniate. Proceedings of the Section of Sciences of the Royal Academy, Amsterdam, 39, 241–252.
- Bonazzi, P., Menchetti, S., Caneschi, A., and Magnanelli, S. (1992) Bottinoite, $\text{Ni}(\text{H}_2\text{O})_6[\text{Sb}(\text{OH})_6]_2$, a new mineral from the Bottino mine, Alpi Apuane, Italy. *American Mineralogist*, 77, 1301–1304.
- Brindley, G.W., and Kao, Chih-Chun (1984) Structural and IR relations among brucite-like divalent metal hydroxides. *Physics and Chemistry of Minerals*, 10, 187–191.
- Busing, W.R., Martin, K.O., and Levy, H.A. (1962) ORFLS. Report ORNL-TM-305. Oak Ridge National Laboratory, Tennessee.
- Clark, A.M. (1993) Bottinoite, a mineral new to Britain. *Mineralogical Magazine*, 57, 543–544.
- Effenberger, H. (1985) The crystal structure of mammothite, $\text{Pb}_6\text{Cu}_4\text{AlSbO}_2(\text{OH})_{16}\text{Cl}_4(\text{SO}_4)_2$. *Tschermaks Mineralogische und Petrographische Mitteilungen*, 34, 279–288.
- Giuseppetti, G., Mazzi, F., and Tadini, C. (1991) The crystal structure of monoclinic langbanite: $(\text{Mn,Ca,Fe,Mg})_4^{2+}(\text{Mn,Fe})_6^{3+}\text{Sb}^{5+}[\text{O}_{16}(\text{SiO}_4)_2]$. *Neues Jahrbuch für Mineralogie Monatshefte*, 193–211.
- Ibers, J.A., and Hamilton, W.C., Eds. (1974) *International tables for X-ray crystallography*, vol. IV. Kynock, Birmingham, U.K.
- Moore, P.B. (1970) Manganostibite: A novel cubic close-packed structure type. *American Mineralogist*, 55, 1489–1499.
- Moore, P.B., and Araki, T. (1976) Bahianite, $\text{Al}_2\text{Sb}_3^{3+}\text{O}_{14}(\text{O,OH})_2$, a novel hexagonal close-packed oxide structure. *Neues Jahrbuch für Mineralogie Abhandlungen*, 126, 113–125.
- North, A.C.T., Phillips, D.C., and Mathews, F.S. (1968) A semiempirical method of absorption correction. *Acta Crystallographica*, A24, 351–359.
- Robinson, K., Gibbs, G.V., and Ribbe, P.H. (1971) Quadratic elongation: A quantitative measure of distortion in coordination polyhedra. *Science*, 172, 567–570.
- Süsse, P., and Tillmann, B. (1987) The crystal structure of the new mineral richelsdorfite, $\text{Ca}_2\text{Cu}_3\text{Sb}(\text{Cl}/(\text{OH})_6/(\text{AsO}_4)_2) \cdot 6\text{H}_2\text{O}$. *Zeitschrift für Kristallographie*, 179, 323–334.
- Tillmanns, E., Krupp, R., and Abraham, K. (1982) New data on the mercury antimony mineral shakhovite: Chemical composition, unit cell and crystal structure. *Tschermaks Mineralogische und Petrographische Mitteilungen*, 30, 227–235.
- Zigan, F., and Rothbauer, R. (1967) Neutronbeugungsmessungen am Brucit. *Neues Jahrbuch für Mineralogie Monatshefte*, 137–143.

MANUSCRIPT RECEIVED DECEMBER 18, 1995

MANUSCRIPT ACCEPTED JULY 12, 1996